Phosphate residues of antigenomic HDV ribozyme important for catalysis that are revealed by phosphorothioate modification†

Jan Wrzesinski,[a] Agnieszka Wichłacz,[a] Danuta Nijakowska,[a] Beata Rebowska,[b] Barbara Nawrot[b] and Jerzy Ciesiołka*[a]

Received (in Montpellier, France) 2nd December 2009, Accepted 19th March 2010
First published as an Advance Article on the web 15th April 2010
DOI: 10.1039/b9nj00727j

The aim of our study was to obtain new details on the role of phosphate residues in antigenomic hepatitis delta virus (HDV) ribozyme for the development of metal ion binding sites and their participation in the cleavage mechanism. In these studies, the wild-type ribozyme and four *in vitro* selected variants, R37, R20, R25 and R51, were used. The application of nucleotide phosphorothioates and the NAIM (nucleotide analog interference mapping) technique for the *cis*-acting ribozymes, wild-type, R25 and R51, revealed the importance of the J4/2 and P1.1 regions in the catalysis. Interestingly, in the wild-type ribozyme, the largest interference effects were observed close to catalytic C76 in the presence of Ca^{2+}, while in the case of Mg^{2+} were in the structurally important helix P1.1. The results obtained for R25 and R51 suggest different coordination of the divalent ions to the phosphate residues within the ribozyme catalytic core. Additionally, replacing the non-bridging oxygen atoms on sulfur in a phosphate group at the cleavage site in *trans*-acting ribozyme variants showed that interactions between pro-R_P and pro-S_P oxygen atoms, and catalytic metal ions, had moderate effects on the cleavage reaction. In the wild-type ribozyme, the ratio of S_P/R_P isomer cleavage rates decreased from 25 for Mg^{2+}-induced cleavage to *ca.* 4 when thiophilic Mn^{2+} or Cd^{2+} were added; thus a "rescue effect" was observed. Interestingly, the R37, R20, R25 and R51 ribozymes showed a reduced R_P/S_P ratio of cleavage rates and much smaller "rescue effects". This suggests that the binding of divalent metal ions in the vicinity of the phosphate group at the cleavage site is very sensitive to the overall ribozyme structure.

Introduction

The hepatitis delta virus (HDV) is a small circular RNA virus that replicates *via* a double rolling circle mechanism. During replication, two viral strands are synthesized, genomic and antigenomic, which contain domains with the self-cleavage activity necessary for processing of both multimeric transcripts into unit-length linear RNAs.[1–3] These domains, with a minimal length of *ca.* 85 nucleotides, are called HDV ribozymes. The products of their self-cleavage reaction end with 5′-OH and 2′,3′-cyclic phosphate groups, indicating that HDV ribozymes utilize the transesterification reaction with a general base–acid mechanism of catalysis.[1–3]

Under physiological conditions, the HDV ribozymes require metal ions for catalytic activity, thus they belong to the metalloenzyme class. Divalent metal ions, including Mg^{2+}, Ca^{2+} and Mn^{2+}, are the most active, but in the presence of Sr^{2+} and Co^{2+}, a low catalytic activity of the ribozymes is also observed.[4] Two different ways of metal ion participation in the cleavage mechanism have been considered.[5,6] In the first, the metals constitute a "glue" that ensures formation of the correct and active ribozyme structure. Magnesium ions are the most effective, however, they can be replaced by monovalents. Indeed, it has been shown that a residual HDV ribozyme catalytic activity is still observed in the presence of a high concentration of monovalent ions (1 M NaCl).[7,8] In the second, a correctly positioned, strongly bound metal ion directly participates in the catalysis. At a pH value close to the pK_a of the metal ion hydrate, it can exist in an ionizable form and may participate in the first step of the transesterification reaction, abstracting a proton from the 2′-OH group of the ribose residue at the cleavage site. A subsequent attack of an O^- nucleophile on the phosphorus atom occurs, and finally the phosphodiester bond is broken. Additionally, other roles postulated for metal ions in the transesterification reaction include the stabilization of the reaction transition state and protonation of the 5′-oxygen leaving group.[5,6]

For the self-cleavage reaction of the genomic HDV ribozyme, a detailed multichannel kinetic model has been proposed, in which each channel involves a different role for Mg^{2+} ions.[7] Channel 1 indicates that divalent ions are not absolutely necessary for folding and catalysis, channel 2 involves a structural Mg^{2+} ion, while channel 3 involves both structural

[a] *Laboratory of RNA Biochemistry, Institute of Bioorganic Chemistry, Polish Academy of Sciences, Noskowskiego 12/14, 61-704 Poznan, Poland. E-mail: ciesiolk@ibch.poznan.pl; Fax: +48 61 8520532; Tel: +48 61 8528503*
[b] *Department of Bioorganic Chemistry, Centre of Molecular and Macromolecular Studies, Polish Academy of Sciences, Sienkiewicza 112, 90-363 Lodz, Poland*
† This paper is dedicated to Professor Wojciech J. Stec on the occasion of his 70th birthday, and is part of a themed issue on Biophosphates.

and catalytic Mg^{2+} ions. The results of subsequent studies[9] have suggested the existence of two different classes of metal ion sites on the genomic HDV ribozyme: a structural site that is inner sphere and shows a preference for Mg^{2+}, and a weak catalytic site that is outer sphere with little preference for a particular divalent metal ion.

The resolution of two different genomic HDV ribozyme crystal structures and numerous biochemical experiments have shown that the ribozyme utilizes base–acid catalysis, involving nucleobases and divalent metal ions.[10,11] The catalytically important C75 nucleobase lies at a hydrogen bonding distance to the 5′-oxygen leaving group and may play the role of a Brønsted acid. In the HDV ribozyme variant deprived of C75 nucleobase, which is completely inactive, the addition of cytosine nucleoside or imidazole rescues the catalytic activity.[12] Thus, a general base–acid catalysis similar to RNase A cleavage of a phosphodiester linkage seems to operate in this ribozyme.[13] An alternative cleavage mechanism has been suggested, in which a hydrated divalent metal ion, observed near the 5′-oxygen leaving group, participates in the reaction as the Brønsted acid.[11] In this mechanism, the C75 residue, located close to the 2′-OH group of the ribose at the cleavage site, plays the role of a general base. Interestingly, similar results have been obtained by molecular dynamic simulations, namely when C75 serves in the catalysis as the Brønsted base and hydrated Mg^{2+} ion as the Brønsted acid.[14]

Generally, metal ions in ribozymes are bound specifically to the functional groups of nucleobases inside ribozyme spatial structures or non-specifically to sugar–phosphate backbones, neutralizing the negative charge of polynucleotide chains.[5] There are several examples of metal ions strongly bound to ribozymes within "metal ion binding pockets". However, the role of ribozyme phosphates in metal ion binding and RNA catalysis is less known. In order to address this problem, a "rescue assay" with respect to sulfur substitution of the non-bridging oxygen atoms in the phosphate group can be applied. In such thio-modified ribozymes, the catalytic activity is strongly reduced in the presence of Mg^{2+}, but can be rescued when thiophilic metal ions Cd^{2+} or Mn^{2+} are added, predicting the presence of a functional metal ion binding site.[15,16] Another approach aimed at the determination of the phosphate groups necessary for the development of metal ion binding sites, or involved in the general base–acid mechanism of cleavage, is nucleotide analog interference mapping (NAIM). This approach utilizes transcription *in vitro* in the presence of 5′-*O*-(1-thio)-nucleoside triphosphates to incorporate thio-modified nucleotides into the RNA chain.[17–20] Subsequently, the RNA is separated into a fraction that has lost its activity and a fraction with an unchanged catalytic function, and in both fractions the sites of thio substitution are determined by an I_2-assisted cleavage. This approach allows the localization of phosphates that interfere with ribozyme function. In the present study, we have applied the NAIM and "metal ion rescue" methods to gain a better understanding of the role of phosphate groups and divalent metal ions in the formation of an active structure, and in the catalysis of antigenomic HDV ribozyme. The wild-type ribozyme and four variants, R37, R20, R25 and R51, obtained previously in our laboratory by an *in vitro* selection approach,[21] were used in our study.

Results

The wild-type antigenomic HDV ribozyme acting *in cis*, and its two sequence variants, R25 and R51 (Fig. 1), were synthesized by an *in vitro* transcription that was carried out in the presence of ATPαS, UTPαS, CTPαS or GTPαS. The thio analogs were incorporated at a level not higher than one modification per molecule. It is important that T7 RNA polymerase incorporates only the S_P-stereoisomer of the phosphorothioate nucleotide modification into RNA chain so as to cause inversion of the configuration at the phosphorus atom, resulting in R_P substitution. Each modified 3′-end-^{32}P-labelled RNA was subjected to a catalytic cleavage promoted by Mg^{2+}, Ca^{2+} or Mg^{2+}. Subsequently, the RNA was separated into a fraction that had lost its activity and a fraction with an unchanged catalytic function, and in both fractions, the sites of thio substitution were determined by an I_2-assisted cleavage (Fig. 2).

Since T7 RNA polymerase accepts only S_P-NTPαS nucleotide analogs, finally yielding R_P-phosphorothioate-modified transcripts, the effects of substitution of the pro-S_P oxygens on sulfur escape the NAIM analysis. In order to evaluate the effect of thio substitution at the phosphate, where the catalysis takes place, two 20-mer oligoribonucleotides were chemically synthesized containing a stereodefined R_P- and S_P-phosphorothioate modification at the putative cleavage site.[22] These oligomers were used as substrates with *trans*-acting versions of HDV ribozymes: wild-type, R37, R20, R25 and R51 (Fig. 1).

Effect of R_P-phosphorothioate modification on the catalytic activity of the wild-type HDV ribozyme

It has been shown that fully phosphorothioate-modified genomic HDV ribozyme was completely inactive, while a partially modified ribozyme proved to be active.[17] Consistently, we showed that the wild-type antigenomic HDV ribozyme variant transcribed with CTPαS at the level of one modification per transcript was catalytically active. The cleavage rate constants (k_{obs}) were 0.60 min^{-1} for Ca^{2+}-, 0.44 min^{-1} for Mg^{2+}- and 0.79 min^{-1} for Mn^{2+}-induced cleavage at metal ion concentrations of 1 mM. These k_{obs} values are *ca.* 1.5-fold lower in the case of the first two metal ions, and even slightly higher for Mn^{2+} in comparison with those determined for the unmodified HDV ribozyme. Here, we present data from the NAIM experiments, showing which pro-R_P non-bridging oxygen atoms of phosphodiester bonds interfere during the RNA catalysis. The experiments were performed using 1 mM Mg^{2+}, Ca^{2+} or Mn^{2+} ions (Fig. 3).

The strongest interference effect for Mg^{2+}-induced cleavage was localized in the J4/2 region at position U77, and was accompanied by a weaker signal at adjacent positions A78/A79 (Fig. 3, panel WT). Additionally, weak interference effects in the P1.1 helix (positions G40/G41/G42 and C24/C25 in the opposite strand of the helix), as well as single interferences in the L4 loop and P4 region, are found. Generally, for the Ca^{2+}-induced cleavage reaction, interference values were higher and two strong signals were present at C76 and U77. Interferences of lower intensity were observed at purine residues G74/G75, A78/A79 and at A20. In the case of

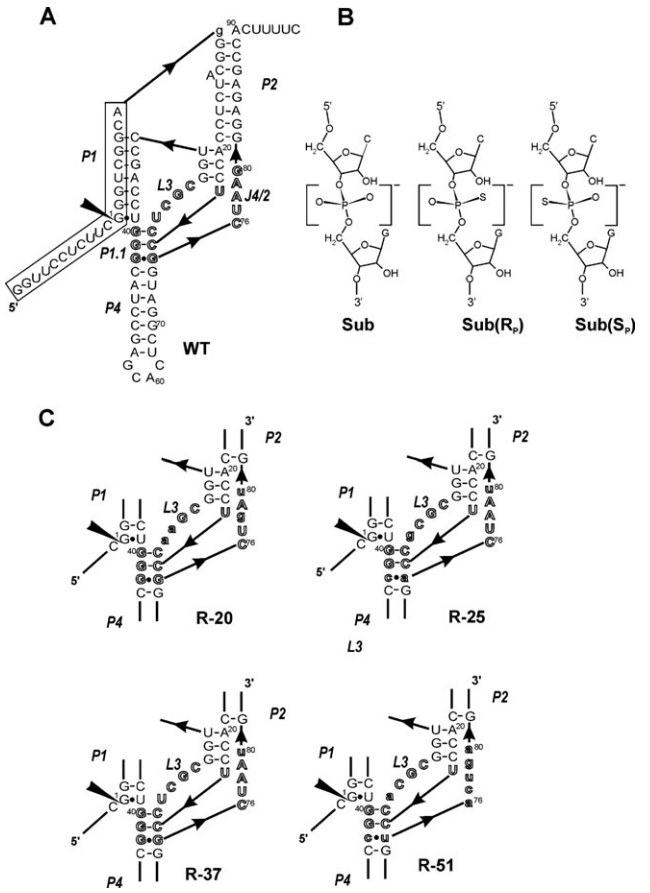

Fig. 1 **A**: A secondary structure model of *cis*-acting antigenomic HDV ribozyme. The model is derived from the consensus HDV ribozyme pseudoknot structure. In the case of the *trans*-acting ribozyme, the boxed sequence was deleted and 20-mer oligoribonucleotide substrates used. The arrow indicates the cleavage site. The outlined fonts denote nucleotides of the ribozyme catalytic core that were randomized in an *in vitro* selection experiment, from which the ribozyme variants shown in panel **C** originate. **B**: The R_P and S_P-phosphorothioate isomers. **C**: The structure of the catalytic core of antigenomic HDV ribozyme variants. Nucleotides different from those found at the corresponding positions of the wild-type sequence are shown in lower case letters.

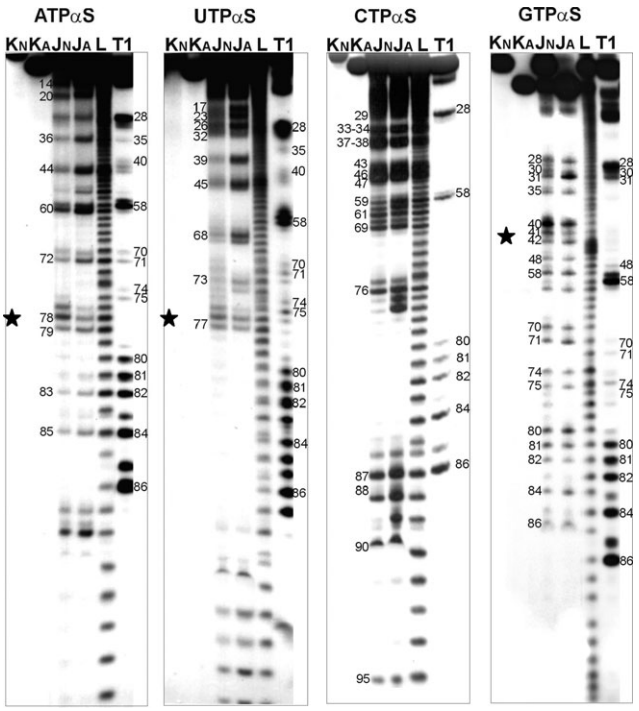

Fig. 2 Iodine cleavage analysis of phosphorothioate-modified 3′-^{32}P-labelled wild-type antigenomic HDV ribozyme. The ribozyme cleavage reaction was carried out in the presence of 1 mM Mg^{2+}. Lanes: K_N, K_A, reaction controls; J_N, J_A, iodine cleavage of the non-active and active fractions of the HDV ribozyme, respectively; L, formamide ladder; T1, limited hydrolysis by RNase T1. Guanosine residues are labelled on the right. The numbers on the left denote phosphorothioate-modified nucleotides. Asterisks indicate regions in which the highest interference effects were observed.

the Mn^{2+}-induced reaction, the strongest interference effects occurred at U77 and A78/A79. Comparing the interference values (κ) at U77, the highest value was observed for Ca^{2+} ($\kappa = 2.7$), moderate for Mg^{2+} ($\kappa = 1.7$) and the lowest value for cleavage induced in the presence of Mn^{2+} ($\kappa = 1.3$). Interference values at A78/A79 were generally smaller and amounted to $\kappa = 1.7$, 1.3 and 1.3 for Ca^{2+}, Mg^{2+} and Mn^{2+}, respectively. In the tertiary structure of the genomic HDV ribozyme, A78 and A79 were located in the vicinity of nucleotides of helix P3, and they together formed a folding motif–ribose zipper region.[10]

In the antigenomic ribozyme, two adenosine residues (A78 and A79) that were possibly involved in the formation of the ribose–zipper motif, were also strongly conserved. However, one HDV isolate was found with guanosine in position 78.[23] Interestingly, we also identified an A78G mutation in some antigenomic ribozyme variants, which were selected *in vitro*.[21] This mutation also occurred in the ribozyme variants R20 and R51, which were analyzed in this study. A guanosine residue is present at position 78 in R20, or in the structurally equivalent position 79 in R51. In our earlier studies, we showed that variant R51 seems to prefer Mg^{2+} in catalysis, unlike the R25 ribozyme, which prefers Mn^{2+}.[21]

It has been postulated that C76 (C75 in the genomic HDV ribozyme) is directly involved in catalysis. Interestingly, replacement of a non-bridging oxygen atom on sulfur in the 5′-position adjacent to the phosphate residue had a moderate interference effect ($\kappa = 1.9$) only for Ca^{2+}-induced cleavage. In the case of Mg^{2+} and Mn^{2+}, there were no interference effects in this position. Low interference values ($\kappa < 1.4$) were observed for nucleotides C24/C25 and G40/G41/G42, although these effects occurred only in the presence of Mg^{2+}. In the crystal structure of the genomic HDV ribozyme, these nucleotides form a pseudoknot motif P1.1, being part of the catalytic core, and they are necessary for ribozyme activity.[10,11]

Interference effects for R_P-phosphorothioate-modified HDV ribozyme variants

Interference experiments with the R25 and R51 ribozymes were performed in the presence of 10 mM concentrations of Mg^{2+}, Ca^{2+} and Mn^{2+} due to the relatively low catalytic activity of these variants.[21] In comparison to the wild-type HDV ribozyme, in variant R25, interference effects

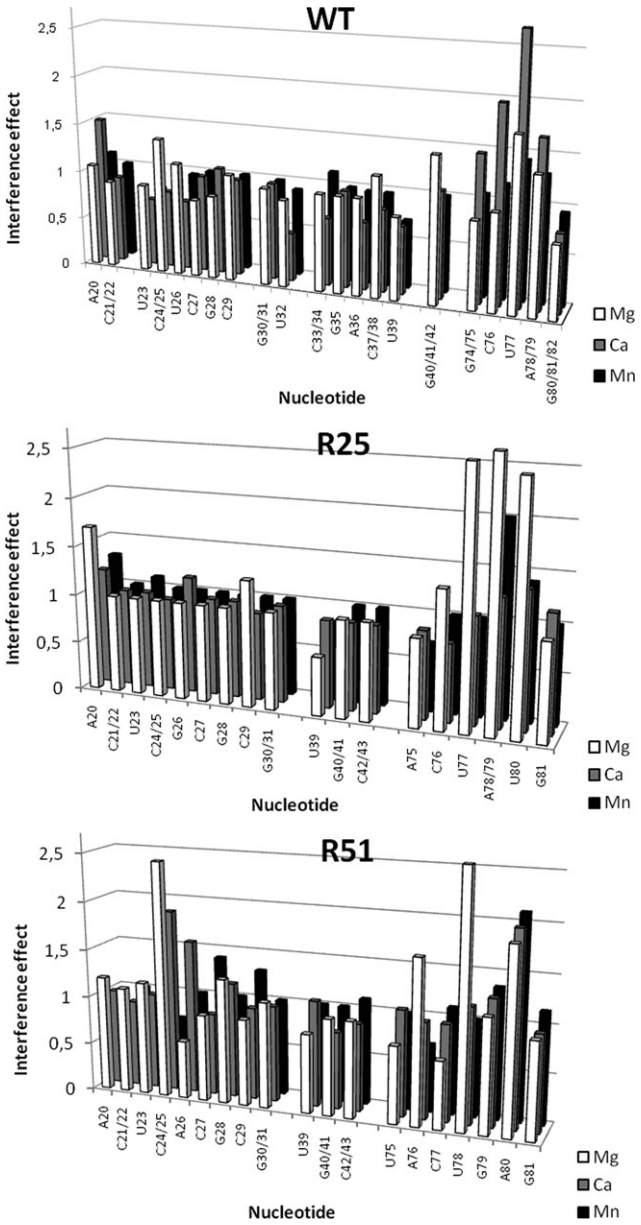

Fig. 3 Interference effects of phosphorothioate-modified wild-type antigenomic HDV ribozyme, and its R25 and R51 sequence variants. Catalytic cleavage was induced by three divalent metal ions: Mg^{2+}, Ca^{2+} and Mn^{2+}. The NAIM experiments were performed using 1 mM divalent metal ions for the wild-type ribozyme and 10 mM ions for the R25 and R51 ribozyme variants. Only regions in which interference effects occurred are shown. The presented data are means of 2–3 independent experiments, and the interference values differed by no more than 10%.

disappeared in helix P1.1 (Fig. 3, panel R25). Most strikingly, strong interferences ($\kappa > 2$) were seen at U77, A78/A79 and at U80 in the J4/2 region in the presence of Mg^{2+}. An additional phosphorothioate interference site is localized at position A20 ($\kappa = 1.7$) in helix P3. In the presence of Ca^{2+}, weak interference signals were observed in the J4/2 region at A78/79 and U80. For Mn^{2+}, strong interference effects were observed at nucleotides A78/A79 ($\kappa = 2.0$) and weaker effects occurred at U80 and A20 ($\kappa = 1.3$–1.4).

In the case of the R51 ribozyme, strong interference signals were seen in the J4/2 region, and unlike in the R25 variant, they were also present in helix P1.1 (Fig. 3, panel R51). Unexpectedly, in the J4/2 region, there were no effects at nucleotides C77 and G79. The catalytic reaction in the presence of Mg^{2+} revealed that non-bridging oxygen atoms of phosphate residues of U78 ($\kappa = 2.5$) and C24/C25 ($\kappa = 2.4$) were very important for the catalysis. Additionally, a moderate effect occurred at A76 ($\kappa = 1.7$), which was not observed in this position in the wild-type HDV ribozyme. For the Ca^{2+}-induced cleavage reaction, phosphate residues at C24/C25 in helix P1.1 ($\kappa = 1.9$) and at A80 in the J4/2 region ($\kappa = 2.0$) seem to be important. Also, an inference effect was observed at A26 in loop P3. For Mn^{2+}-induced catalysis, strong interference was seen at A80 ($\kappa = 2.0$), the only signal in the J4/2 region.

Phosphorothioate modification at the antigenomic HDV ribozyme cleavage site

In order to analyze the effect of thio substitution in the phosphate residue at the cleavage site on cleavage kinetics and efficiency, we applied *trans*-acting antigenomic HDV ribozymes: wild-type and its four sequence variants R37, R20, R25 and R51 (Fig. 1). Two 20-mer oligoribonucleotides were used as ribozyme substrates with stereo-defined R_P- and S_P-phosphorothioate substitutions at the cleavage site. Cleavage reactions were performed in the presence of three divalent metal ions with different chemical properties. "Hard" metal ion Mg^{2+} binds preferentially to oxygen atoms whereas "soft" thiophilic metal ions Mn^{2+} and Cd^{2+} coordinate with relatively high affinity to sulfur atoms.[16] For example, for ATPβS, the Mg^{2+} ion binds 30 000-fold more strongly to oxygen than to sulfur, while binding of Mn^{2+} to oxygen and to sulfur is almost equal.[24]

If "hard" and "soft" metal ions occupy the same binding pocket inside the ribozyme structure and metal ions participate in the cleavage mechanism, such an unmodified ribozyme will show catalytic activity in the presence of Mg^{2+}, while the activity for the R_P-phosphorothioate-modified ribozyme will be reduced. However, the catalytic activity of an R_P-phosphorothioate-modified ribozyme may be rescued when thiophilic metal ions (Mn^{2+}, Cd^{2+}) are used. In the case of hammerhead ribozyme, only the S_P-phosphorothioate-modified substrate is cleaved in the presence of Mg^{2+}. The addition of Cd^{2+} restores the catalytic activity of the R_P-isomer without influencing the cleavage rate of the S_P-isomer.[15,16] This observation is good evidence of metal ion participation in the cleavage mechanism, occurring in the hammerhead ribozyme.[25]

We found that in the presence of a 1 mM concentration of Mg^{2+} and Mn^{2+}, the *trans*-acting wild-type HDV ribozyme and R37 variant were cleaved with similar rates (data not shown). Preliminary experiments with thio-modified oligoribonucleotide substrates showed that the R_P-substrate was cleaved with a 6-fold and the S_P-isomer with an approximately 15-fold lower cleavage rate than the unmodified oligomer, both in the presence of Mg^{2+} and Mn^{2+} ions. Moreover, in the presence of 1 mM Cd^{2+}, the unmodified oligomer was

completely inactive. The thio-modified oligomers were cleaved with relatively low efficiency, and the cleavage extents did not exceed 10% after 60 min. For the other ribozyme variants, R25, R20 and R51, the k_{obs} values were 40–60-fold lower than for the wild type ribozyme (data not shown). Therefore, we decided to perform subsequent experiments in the presence of Mg^{2+}, Mn^{2+} and Cd^{2+} at a 10 mM concentration. The *trans*-acting ribozymes with 20-mer oligonucleotide substrates were cleaved under single turnover conditions (the ribozymes were used in high excess over the substrates), and the reactions were approximated to pseudo first-order kinetics.

We carried out classical rescue experiments using a 10 mM concentration of metal ions: 10 mM Mg^{2+}, as well as 9 mM Mg^{2+} supplemented with 1 mM thiophilic metal ions: Mn^{2+} and Cd^{2+} (Table 1). Briefly, the presence of Mg^{2+} ensured proper folding of the ribozymes, while the addition of thiophilic Mn^{2+} and Cd^{2+} showed whether the reduced cleavage activity of the thio-substituted ribozymes in Mg^{2+} could be rescued, predicting the presence of a functional metal–ion binding site. The observed cleavage rates were significantly higher than those in the presence of 1 mM of divalent metal ions. In the case of wild-type HDV ribozyme, the k_{obs} values were similar for the Mg^{2+}-, Mn^{2+}- and Cd^{2+}-induced reactions with both substrates, the unmodified and the S_P derivatives. However, the ratio of the cleavage rate constants for the S_P and the R_P isomers was 25 in the presence of Mg^{2+}. The catalytic activity of the R_P-isomer was partly rescued when additional thiophilic Mn^{2+} or Cd^{2+} was present at a 1 mM concentration. The ratio of the cleavage rates decreased to *ca.* 4, in both cases. Unexpectedly, the R37 ribozyme showed a lower interference effect, and the ratio of the cleavage rates for the S_P and R_P thio substrates amounted to 6.4 in the presence of Mg^{2+}. When Mn^{2+} or Cd^{2+} were present in the cleavage buffer, the ratio dropped to *ca.* 4, a value similar to that observed for the wild-type ribozyme.

The R20, R25 and R51 ribozymes were less active than the wild-type and R37 variants (Table 1). For R25, the ratio of the cleavage rate constants for the S_P and R_P isomers in the presence of Mg^{2+} was basically identical to the one determined for the R37 variant, although the k_{obs} values were 20-fold lower. Cleavage reactions in the presence of thiophilic Mn^{2+} or Cd^{2+} showed a rescuing of the catalytic activity. Interestingly, in the case of the R20 variant, the ratio of the cleavage rate constants for the S_P and R_P thio substrates was almost identical for all of the studied metal ions. The R51 ribozyme showed a low catalytic activity, and the thio substrate with an R_P configuration was not cleaved in the presence of Mg^{2+}.

Discussion

The aim of our studies was to obtain new information on the role of phosphate residues in antigenomic HDV ribozyme, in the development of metal ion binding sites and participation in the cleavage mechanism. The application of nucleoside phosphorothioates and the NAIM method, to compare the location of phosphorothioate interference sites in the cleaved and non-cleaved ribozyme fractions, revealed the importance of the J4/2 and P1.1 regions in the catalysis. Although these regions seemed to be crucial in the wild-type ribozyme or in ribozyme variants R25 and R51, substantial differences in the location of interference effects and their relative intensities were observed, depending which variant and metal ion were used in the cleavage reaction.

In the wild-type ribozyme, the non-bridging oxygen atoms located at neighboring positions G74, G75, C76 and U77 in the J4/2 region had the highest interference values for Ca^{2+}-induced catalytic cleavage. Such an observation confirms previous suggestions that HDV ribozymes have exceptional metal ion specificity and are active in the presence of Ca^{2+}, in contrast to other natural ribozymes, which show

Table 1 The influence of phosphorothioate modification at the catalytic cleavage site in *trans*-acting antigenomic HDV ribozymes on cleavage rate constants (k_{obs}) in the presence of Mg^{2+}, Mn^{2+} and Cd^{2+} ions[a]

	10 mM Mg^{2+} $k_{obs} \times 10^3/min^{-1}$ Ep (%)	9 mM Mg^{2+} + 1 mM Mn^{2+} $k_{obs} \times 10^3/min^{-1}$ Ep (%)	9 mM Mg^{2+} + 1 mM Cd^{2+} $k_{obs} \times 10^3/min^{-1}$ Ep (%)
WT			
Sub	378.4 ± 11.7 (85)	827.6 ± 116.4 (76)	350.7 ± 23.0 (92)
S_P	376.9 ± 11.9 (83)	615.6 ± 16.9 (85)	245.6 ± 19.1 (81)
R_P	15.1 ± 3.7 (10) *25.0*	135.2 ± 14.5 (25) *4.6*	57.0 ± 1.0 (19) *4.3*
R37			
Sub	453.3 ± 4.32 (82)	488.8 ± 11.2 (82)	455.0 ± 14.4 (91)
S_P	394.1 ± 14.0 (80)	501.6 ± 10.9 (81)	397.2 ± 14.9 (78)
R_P	61.2 ± 1.77 (15) *6.4*	109.6 ± 6.8 (19) *4.6*	102.0 ± 7.0 (17) *3.9*
R25			
Sub	20.7 ± 0.5 (24)	30.6 ± 1.2 (51)	25.0 ± 0.9 (54)
S_P	19.2 ± 1.0 (19)	17.8 ± 7.4 (35)	15.9 ± 1.1 (27)
R_P	3.1 ± 0.2 (2) *6.2*	7.1 ± 0.4 (11) *2.5*	12.4 ± 2.3 (20) *1.3*
R20			
Sub	7.8 ± 0.1 (32)	51.1 ± 1.7 (82)	11.2 ± 0.3 (33)
S_P	8.9 ± 0.4 (20)	22.7 ± 1.3 (59)	6.9 ± 0.1 (30)
R_P	5.4 ± 0.3 (11) *1.6*	9.9 ± 0.3 (15) *2.3*	7.0 ± 1.0 (7) *1.0*
R51			
Sub	0.9 ± 0.1 (5)	4.5 ± 0.1 (7)	1.8 ± 0.4 (10)
S_P	3.7 ± 0.2 (4)	4.2 ± 0.1 (3)	1.1 ± 0.2 (8)
R_P	0 (0)	2.0 ± 0.3 (2) *2.1*	1.9 ± 0.8 (5) *0.6*

[a] The S_P/R_P ratio of the cleavage rates is shown in italics; Ep denotes the ribozyme fraction cleaved after 60 min.

Mg^{2+} specificity.[1,21,23] At U77, a strong interference effect was detected in the presence of Ca^{2+}, a little lower in Mg^{2+} and weak in Mn^{2+}. In a cross-linking experiment of *trans*-acting antigenomic HDV ribozyme, U77 formed a dimer with the base in position −1 of the substrate.[26] It has been suggested that these interactions play an important role in ribozyme folding into catalytically active structures.[27] It is possible that the replacement of the oxygen atom for sulfur at U77 affected RNA folding, influencing in turn the catalytic activity of the ribozyme. In the genomic HDV ribozyme, G76, a counterpart of U77 in the antigenomic variant, is a member of the trefoil turn motif, which involves nucleotides G74, C75 and G76. This motif ensures the correct position of C76 close to the cleaved phosphodiester bond.[10,11] Additionally, two Mg^{2+} ions stabilize the motif structure, where phosphorothioate interferences occurred at A78 and A79. In the genomic HDV ribozyme, these bases form a ribose zipper motif and are necessary for catalysis, since any mutation in these positions dramatically reduces the ribozyme activity.[23] Interestingly, the NAIM analysis also revealed interference signals at A20, in a position occupied by G20 in the genomic variant, which in the crystal structure interacts with a closely located A78 and A79 motif.[10,11] Thus, the observed phosphorothioate interference confirms that phosphate residues of the ribose zipper motif may also play an important role in the catalysis. This conclusion is supported by the results of the NAIM analysis of the R51 ribozyme variant. In this ribozyme, a guanosine residue is present in position 79, which is structurally equivalent to A78 in the genomic HDV ribozyme. This may influence the possibility of forming the ribose zipper motif and binding of metal ions in the vicinity. These changes are reflected in the patterns of phosphorothioate interference for the R51 ribozyme in the region J4/2, which are substantially different from those observed for the wild-type ribozyme (Fig. 3).

Interferences in the P1.1 helix, a pseudoknot structure formed by C24–G40 and C25–G41 base pairs, were found only in the wild-type ribozyme in the presence of Mg^{2+}. This strongly suggests that this motif coordinates Mg^{2+} ions. In the crystal structure of genomic HDV ribozyme, two non-bridging oxygen atoms of C21 and C22 are involved in the development of the P1.1 helix. In the pre-cleavage state, Mg^{2+} interacts with pro-R_P C22 nucleobase (C25 in the antigenomic variant); however, in the post-cleavage state with no Mg^{2+} ion, pro-R_P-O C21 (C24 in antigenomic variant) interacts with the N4 atom of the catalytic C75 nucleobase (C76 in antigenomic variant).[10,11] Since phosphorothioate interferences were found at C24 and C25, as well as at C76, in the antigenomic HDV ribozyme, the NAIM results support the proposed similar cleavage mechanism pathway in both HDV ribozymes.

In an earlier NAIM study[17] of the genomic HDV ribozyme, a relatively high level of thio substitution (*ca.* 20% NMPαS per precursor) was employed and catalytic cleavage occurred during *in vitro* transcription in the presence of 6 mM Mg^{2+}. The highest values of phosphorothioate interference were detected at G1 at the cleavage site, at C21 in the L3 loop and at G40 in the J1/4 region. In another study,[18] a variant of genomic HDV ribozyme was used, in which a significant section of stem IV was deleted. The ribozyme was thio-substituted at the level of one phosphorothioate per molecule, and interference effects were analyzed after catalytic cleavage in the presence of either 6 or 15 mM Mg^{2+}. The interference signals were clustered into three distinct regions, L3, J1/4 and J4/2, which are important in the catalysis.[18]

Clustering of phosphorothioate interference sites in regions important in catalysis in other natural ribozymes have also been observed. In the CPEB3 ribozyme, which seems to be structurally and functionally related to the HDV ribozyme, interferences have been found in regions corresponding to P1.1 and J4/2.[28] The authors claim that such an observation is good evidence for the evolutional similarity of both ribozymes, and for the idea that the CPBE3 ribozyme is an "ancestor" of the HDV ribozyme. In *E. coli* RNase P RNA, sites of phosphorothioate interference are located in helix P4.[29] In *Tetrahymena* ribozyme, catalytically important pro-R_P oxygen atoms in the region of helix P7 have been clustered.[30] In conclusion, the clustering of R_P-phosphorothioate interferences in sites important for catalysis indicates the importance of phosphate groups of the polynucleotide chain in RNA catalysis.

The replacement of non-bridging oxygen atoms for sulfur at the cleavage site of antigenomic HDV ribozyme showed that interactions between the pro-R_P and pro-S_P oxygen atoms and catalytic divalent metal ions had moderate effects on the cleavage reaction. The ratio of the S_P/R_P isomer cleavage rates decreased from 25 for Mg^{2+}-induced cleavage to *ca.* 4 for cleavage in the presence of additional Mn^{2+} or Cd^{2+} ions (Table 1). Interestingly, all the other ribozyme variants showed a reduced R_P/S_P ratio of cleavage rates, even including the R37 variant, which contains the single mutation G80U. Moreover, in these variants, the "rescue effects" were much smaller than the effect observed for the wild-type ribozyme. This suggests that divalent metal ions, which are bound in the vicinity of phosphate pro-R_P and pro-S_P oxygen atoms at the cleavage site, are very sensitive to the overall ribozyme structure. It also confirms previous suggestions that the wild-type antigenomic HDV ribozyme is best suited for catalysis.[21,31]

In the *trans*-acting genomic HDV ribozyme, the substitution of sulfur for the R_P-oxygen and the S_P-oxygen at the cleavage site of the substrate had no effect on the rate constant, although the amounts of catalytically-active complex were different.[32] Two possibilities have been suggested to explain the absence of any significant "thio effect". The rate-limiting step of the reaction may be the step at which a conformational change occurs prior to the cleavage reaction, rather than the chemical cleavage step. Alternatively, the thio substitution affects the coordination of the metal ion but does not influence the chemical cleavage step. Moreover, no significant "Mn^{2+} rescue effect" was observed, and the authors suggest that Mg^{2+} ions do not interact directly with the pro-R_P oxygen, but are essential to the formation of the active ribozyme complex.[32]

The results of the "rescue experiment" for the antigenomic HDV ribozyme suggested the participation of divalent metal ions in the cleavage mechanism. However, a comparison of the "rescue effects" for the antigenomic HDV ribozyme and those described earlier for other ribozymes revealed essential differences in the presence of Cd^{2+}.[15,16,25] In the hammerhead

and RNase P ribozymes, the catalytic activity was fully recovered in the presence of a micromolar concentration of Cd^{2+}; however, in the antigenomic HDV ribozyme, such an effect did not occur. Presumably, in this ribozyme, the metal ion binding site has a low affinity for Cd^{2+}, in contrast to other ribozymes. Metal ion binding pockets in ribozymes are usually characterized by a relatively broad specificity.[5,6] However, in some cases, the coordination of metal ions is more selective and is strongly influenced by any changes in the ribozyme structure. For example, comparative studies of seven different hammerhead ribozymes showed that even a small change in oligonucleotide substrate length from 8 to 10 nucleotides dramatically influenced the "rescue effect" from 18 000 to 50.[25]

Conclusions

The application of nucleoside phosphorothioates and the NAIM method to compare the location of phosphorothioate interference sites in cleaved and non-cleaved fractions of the antigenomic HDV ribozyme revealed the importance of phosphate groups of the J4/2 and P1.1 regions in the catalysis. Interestingly, in the wild-type ribozyme, the largest interference effects were observed close to catalytic C76 in the presence of Ca^{2+}, while in the case of Mg^{2+} it was in the structurally important helix P1.1. The phosphate groups of the J4/2 and P1.1 regions also seem to be crucial to the catalysis in ribozyme sequence variants R25 and R51, which were earlier selected *in vitro*. However, substantial differences in the location of the interference effects and their relative intensities were observed for these ribozymes, depending on which variant and metal ion were used in the cleavage reaction. This suggests the different coordination of divalent ions to phosphate residues within the ribozyme catalytic core.

Additionally, replacing the non-bridging oxygen atoms for sulfur in a phosphate group at the cleavage site in the *trans*-acting antigenomic HDV ribozyme showed that interactions between the pro-R_P and pro-S_P oxygen atoms and catalytic metal ions had moderate effects on the cleavage reaction. In the wild-type ribozyme, the ratio of S_P/R_P isomer cleavage rates decreased from 25 for the Mg^{2+}-induced cleavage to *ca.* 4 when thiophilic Mn^{2+} or Cd^{2+} were added; thus, a "rescue effect" was observed. Interestingly, the *in vitro*-selected ribozyme variants R37, R20, R25 and R51 showed a reduced R_P/S_P ratio of cleavage rates and much smaller "rescue effects". This suggests that divalent metal ions, which are bound in the vicinity of phosphate pro-R_P and pro-S_P oxygen atoms at the cleavage site, are very sensitive to the overall ribozyme structure.

Experimental

Materials

Phosphorothioate nucleotides (NTPαS) were purchased from Glen Research. T7 RNA polymerase, DNA Taq polymerase, T4 polynucleotide kinase and RNA ligase were from MBI Fermentas. (γ-^{32}P) ATP (5000 Ci mmol^{-1}) was from Hartmann Analytic. Chemicals were purchased from Serva or Fluka.

Synthesis of R_P and S_P phosphorothioate-modified oligoribonucleotides

P-stereodefined oligonucleotide phosphorothioates of the following sequence 5′-CUUUCCUCUUC$_{PS}$GGGUCGGCA-3′ were prepared according to a recently described procedure.[22] Briefly, P-stereodefined diribonucleoside ($C_{PS}G$) phosphorothioates were obtained using diastereomerically pure 2-thio-1,3,2-oxathiaphospholane 5′-DMT-2′-TOM-cytidine monomers, protected at the sulfur atom and phosphitylated with *O*-2-cyanoethyl-*N*,*N*,*N*′,*N*′-tetraisopropylamidophosphite in the presence of 2-ethylthio-1*H*-tetrazole. The resulting monomers, together with the phosphoramidite derivatives of four common nucleosides, were used for the automated synthesis of oligoribonucleotides by the phosphoramidite approach. The resulting solid support-bound oligonucleotides were subjected to DMT group removal and, after the cleavage from the support oligonucleotides, were deprotected, precipitated with n-butanol, purified by reverse phase HPLC and de-salted on SepPak cartridges (Waters). MALDI-TOF MS analysis confirmed the structure of the resulting oligonucleotides: Calc. MW 6288, R_P-PS-oligonucleotide: m/z 6289, S_P-PS-oligonucleotide: m/z 6285.

DNA template constructs

The dsDNA templates for the *in vitro* transcription of HDV ribozymes were prepared as follows. For the *trans*-acting ribozymes: wild-type, R20, R25, R37 and R51 two DNA oligomers were synthesized: oligomer A1, 5′-GAAAAGTGGC-TCTCC(CTTAGC) CATCCGAGTGCTCGGATG(CCC)AG-GTCGGACC(GCGAGGA)GGTGGAGATGCCC-3′ and oligomer B1, 5′-*TAATACGACTCACTATA*GGGCATCT-CCACC-3′. For the *cis*-acting ribozymes: wild type, R25 and R51, oligomer A1 and oligomer B2, 5′-*TAATACGACT-CACTATAG*GGTCCTCTTCGGGTCGGCAGGGCATCT-CCACC-3′ were used (in the oligomer A1, letters in parentheses denote nucleotides of the wild-type sequence, which were changed to appropriate residues present in the ribozyme variants, as shown in Fig. 1; in both oligomers, the complementary sequences are underlined, and in oligomers B1 and B2, letters in italics mark the T7 RNA polymerase promoter). Equimolar amounts of both pairs of oligomers (A1–B1 or A1–B2) were annealed. The reaction mixture contained 1.5 μM A1–B1 or A1–B2 oligomers, 10 mM Tris-HCl (pH 7.0), 2 mM $MgCl_2$, 150 mM KCl, 0.1% Triton X-100, 200 μM of each dNTP and 60 units ml^{-1} of DNA Taq polymerase. The reaction was performed on a Biometra UNO II thermocycler for six cycles, 30 s at 93 °C, 30 s at 55 °C and 1 min at 72 °C. The mixtures were extracted with phenol/chloroform (1 : 1), and the DNA was precipitated with ethanol at −20 °C overnight. The dsDNA template was recovered by centrifugation, dissolved in TE buffer and used in the transcription reaction.

Synthesis of *trans*-acting ribozymes

The *in vitro* transcription reaction was performed using 0.5 μM dsDNA template, 40 mM Tris-HCl (pH 8.0), 10 mM $MgCl_2$,

0.001% Triton X-100, 2 mM spermidine, 5 mM DTT, 1 mM of each NTP, 750 U ml^{-1} RNase inhibitor and 2000 U ml^{-1} T7 RNA polymerase. The transcription mixture was incubated at 37 °C for 4 h. Subsequently, the transcription products were precipitated and purified by electrophoresis on 8% polyacrylamide gels containing 1 mM EDTA and 7 M urea. The band corresponding to the ribozyme was localized by UV shadowing, cut out and the RNA eluted from the gel with 0.3 M sodium acetate (pH 5.2), 1 mM EDTA, ethanol precipitated and dissolved in sterile water containing 0.1 mM EDTA.

Preparation of phosphorothioate-modified ribozymes

The phosphorothioate-modified *cis*-acting ribozymes were prepared by *in vitro* transcription using the same reaction conditions as described for the *trans*-acting variants. Additionally, the reaction mixtures contained one of the following phosphorothioate analogs: 0.07 mM ATPαS, 0.07 mM UTPαS, 0.04 mM CTPαS or 0.05 mM GTPαS. The reaction was carried out in the presence of oligomer D20: 5′-GGAGATGCCCTGCCGACCCG-3′ at 4 μM concentration, which prevented ribozyme self-cleavage. Following incubation of the mixtures at 37 °C for 4 h and purification of transcription products on polyacrylamide gels, the modified RNA transcripts were excised, eluted, precipitated with ethanol, the RNA recovered by centrifugation, and dissolved in 10 mM Tris-HCl (pH 7.0) and 0.1 mM EDTA.

Ribozyme cleavage

The *trans*-acting HDV ribozymes were prepared by mixing the 5′-end-^{32}P-labeled oligonucleotide substrates: Sub, 5′-CUUU-CCUCUUCGGGUCGGCA-3′ or Sub (S_P or R_P), 5′-CUUUCCUCUUC_{PS}GGGUCGGCA-3′ (50 000 cpm, 0.1 pmol of RNA in 50 μl reaction volume) with the analyzed ribozyme in a standard reaction buffer of 50 mM Tris-HCl (pH 7.5), 0.1 mM EDTA to obtain a final RNA concentration of <2 nM and 500 nM for the substrate and ribozyme components, respectively. The *cis*-acting 3′-end-^{32}P-labeled ribozymes were tested at a 500 nM concentration of RNA in the same cleavage buffer.

The ribozymes were subjected to a denaturation–renaturation procedure by incubating at 100 °C for 2 min, at 0 °C for 10 min and finally at 37 °C for 10 min. The cleavage reactions were initiated by adding an appropriate divalent metal chloride solution. The reactions proceeded at 37 °C and were quenched with equal volumes of a 20 mM EDTA/7M urea mixture containing electrophoresis dyes. Products of the catalytic cleavage were analyzed by electrophoresis on 12% polyacrylamide, 0.75% bis-acrylamide, 8 M urea gels. For quantitative analysis, radioactive bands were quantified using phosphorimaging screens, the Typhoon 8600 imager and ImageQuant software (Molecular Dynamics). To determine the cleavage rate constant, reaction aliquots were taken at specified time points. The cleavage products were quantified after electrophoretic separation, and subsequently the logarithm of the percentage of the remaining RNA was plotted as a function of time. The negative slope of the least-squares plot yielded the cleavage rate constant.

Nucleotide analogs interference mapping

The *cis*-acting 3′-end-^{32}P-labeled ribozyme was subjected to self-cleavage, and the reaction was terminated when *ca.* half of the initial amount of RNA had been cleaved. After separation on a polyacrylamide gel, the RNA fraction containing molecules that were specifically cleaved in the presence of divalent metal ions (J_A) and the fraction deprived of such properties (J_N) were subjected to cleavage of the phosphorothioate linkages in the presence of a 10 mg ml^{-1} iodine/ethanol solution. The I_2 cleavage was carried out at 37 °C for 15 min. Subsequently, the RNA was precipitated, recovered by centrifugation and dissolved in a loading buffer (7 M urea/dyes, 10 mM EDTA). Patterns of I_2 cleavage were compared on 8 M urea/12% polyacrylamide gels alongside alkaline hydrolysis ladders and partial digestion with RNase T_1. Products were visualized by autoradiography or quantified using a PhosphoImager Typhoon 8600 imager with ImageQuant software. Interference values were calculated from the equation: κ = [(band intensity at nucleotide x)/(Σband intensity at nucleotide a–z)$_{cleaved}$]/[(band intensity at nucleotide x)/(Σband intensity at nucleotide a–z)$_{uncleaved}$]. Interferences were evaluated as follows: weak κ = 1.1–1.5, moderate κ = 1.5–2.0 and strong interferences were assigned values $\kappa > 2.0$. In some cases, interference values were assigned to two (three) adjacent nucleotides when the incomplete separation of bands on polyacrylamide gels precluded the unambiguous calculation of interference effects for single nucleotides.

Acknowledgements

This work was supported by the Polish Ministry of Science and Higher Education (grant no. NN204 161633), and by the Bioorganic Chemistry and Structural Biology Network.

References

1 A. T. Perrotta and M. D. Been, *Nature*, 1991, **350**, 434–436.
2 J. M. Taylor, *Curr. Top. Microbiol. Immunol.*, 2006, **307**, 1–23.
3 J. C. Cochrane and S. A. Strobel, *Acc. Chem. Res.*, 2008, **41**, 1027–1035.
4 J. Wrzesinski, M. Łęgiewicz, B. Smólska and J. Ciesiołka, *Nucleic Acids Res.*, 2001, **29**, 4482–4492.
5 K. O. Sigel and A. M. Pyle, *Chem. Rev.*, 2007, **107**, 97–113.
6 M. Fedor, *Annu. Rev. Biophys.*, 2009, **38**, 271–299.
7 S. Nakano, D. J. Proctor and P. C. Bevilacqua, *Biochemistry*, 2001, **40**, 12022–12038.
8 J. L. O'Rear, S. L. Wang, A. L. Feig, L. Beigelman, O. C. Uhlenbeck and D. Herschlag, *RNA*, 2001, **7**, 537–545.
9 S. Nakano, A. L. Cerrone and P. C. Bevilacqua, *Biochemistry*, 2003, **42**, 2982–2994.
10 A. R. Ferré-D'Amaré, K. Zhou and J. A. Doudna, *Nature*, 1998, **395**, 567–574.
11 A. Ke, A. K. Zhou, F. Ding, J. H. Cate and J. A. Doudna, *Nature*, 2004, **429**, 201–205.
12 A. T. Perrotta, I. Shih and M. D. Been, *Science*, 1999, **286**, 123–126.
13 R. T. Raines, *Chem. Rev.*, 1998, **98**, 1045–1066.
14 P. Banáš, L. Radisek, V. Hanosova, D. Svozil and N. G. Walter, *J. Phys. Chem. B*, 2008, **112**, 11177–11187.
15 T. Takagi, M. Warashina, W. J. Stec, K. Yoshinari and K. Taira, *Nucleic Acids Res.*, 2001, **29**, 1815–1834.
16 V. J. DeRose, *Curr. Opin. Struct. Biol.*, 2003, **13**, 317–324.
17 Y. H. Jeoung, P. K. Kumar, Y. A. Suh, K. Taira and S. Nishikawa, *Nucleic Acids Res.*, 1994, **22**, 3722–3727.

18 N. S. Prabhu, G. Gotlieb and P. A. Gotlieb, *Nucleic Acids Res.*, 1997, **25**, 5119–5124.
19 S. A. Strobel, *Biopolymers*, 1998, **48**, 65–81.
20 S. Kuzic and R. K. Hartmann, in *Handbook of RNA Biochemistry*, ed. R. K. Hartmann, A. Bindereif, A. Schon and E. Westhof, Wiley-VCH GmbH & Co, KGaA, Weinheim, 2005, pp. 294–318.
21 M. Łęgiewicz, A. Wichłacz, B. Brzezicha and J. Ciesiołka, *Nucleic Acids Res.*, 2006, **34**, 1270–1280.
22 B. Nawrot, B. Rebowska, O. Michalak, M. Bulkowski, D. Blaziak, P. Guga and W. J. Stec, *Pure Appl. Chem.*, 2008, **80**, 1859–1871.
23 (*a*) I. H. Shih and M. D. Been, *Annu. Rev. Biochem.*, 2002, **71**, 887–917; (*b*) T. S. Wadkins and M. D. Been, *Cell. Mol. Life Sci.*, 2002, **59**, 112–125.
24 V. L. Pecoraro, J. D. Hermes and W. W. Cleland, *Biochemistry*, 1984, **23**, 5262–5271.
25 E. C. Scott and O. C. Uhlenbeck, *Nucleic Acids Res.*, 1999, **27**, 479–484.
26 J. Ouellet and J. P. Perreault, *RNA*, 2004, **10**, 1059–1062.
27 C. Reymond, J. Quellet, M. Basaillon and J. P. Perreault, *RNA*, 2006, **13**, 44–54.
28 K. Salehi-Ashtiani, A. Luptak, A. Litovchick and J. Szostak, *Science*, 2006, **313**, 1788–1792.
29 W. D. Hardt, J. M. Warnecke, V. A. Erdmann and R. K. Hartmann, *EMBO J.*, 1995, **14**, 2935–2944.
30 E. L. Christian and M. Yarus, *J. Mol. Biol.*, 1992, **228**, 743–758.
31 D. M. Chadalavada, A. L. Cerrone-Szakal and P. C. Bevilacqua, *RNA*, 2007, **13**, 2189–2201.
32 H. Fauzi, J. Kawakami, F. Nishikawa and S. Nishikawa, *Nucleic Acids Res.*, 1997, **25**, 3124–3130.

